RSC Advances

PAPER

View Article Online
View Journal | View Issue

Cite this: *RSC Adv.*, 2019, **9**, 24852

Nitrogen-doped fluorescent carbon dots used for the imaging and tracing of different cancer cells

Tinghua Yan,[a] Wang Zhong,[a] Ruiming Yu,[b] Gao Yi,[b] Zeping Liu,[b] Lihong Liu,[e] Xinxing Wang *[d] and Jinhua Jiang*[c]

Received 28th April 2019
Accepted 31st May 2019

DOI: 10.1039/c9ra03170g

rsc.li/rsc-advances

Here, we report the synthesis of nitrogen-doped fluorescent carbon (C) dots using a one-pot hydrothermal method. Transmission electron microscopy results reveal that the particle size of the nitrogen-doped C-dots is very small, with an average diameter of 4.6 nm. After being kept in water for 10 days, the nitrogen-doped C-dots can still dissolve well in the water, showing good stability and compatibility in aqueous solution. The fluorescence spectra show that the nitrogen-doped C-dots exhibit emission-tunable color from blue to green upon excitation from 230 to 520 nm. Cell tests show that the C-dots are low in cytotoxicity and can be used for imaging, detecting and tracing between hepatoma and HeLa cells, because hepatoma and HeLa cells show different sensitivity to different fluorescent colors pumped at different excitation wavelengths.

1. Introduction

Nowadays, the problems associated with cancer affect millions of people. Although a large number of techniques, such as chemotherapy, hyperthermia and thermochemotherapy,[1–6] have been widely suggested for killing cancer cells, great harm resulting from the unpleasant side effects also greatly impose upon the patients.[7–9] Typically, when the patients are exposed to high energy electrons and chemical conditions for a long time, normal cells are also killed, leading to a variety of other diseases.[9–12] In this case, developing effective, low cost and non-invasive detection methods that can trace and detect cancer cells before disease appearance is of high scientific importance.

In the past years, optical imaging strategies based upon fluorescent materials have been frequently suggested in biological fields. Due to fluorescence behavior, such types of materials can be used as biological techniques for imaging cells. With great efforts made over the past few years, so far tens of thousands of fluorescent materials, the particle size of which spans from the nano to the micro level, have become available for biological imaging purposes, such as fluorescent organic dyes,[13–16] quantum dots (QDs),[15,17–20] polymers,[21–23] two-dimensional (2D) materials,[24–26] mechano-optical converters,[27,28] down-conversion,[29–31] up-conversion,[32–35] and afterglow particles,[36–38] and metal–organic frameworks (MOFs).[39,40] Most of them, however, suffer from either high cytotoxicity and cost (*i.e.* organic dyes and Cd-related QDs), a large particle size (usually micro-size, *i.e.* mechano-optical converters), single emission color (*i.e.* trivalent rare earth-doped phosphor materials), or ultrahigh molecular weight and complicated synthesis processes (*i.e.* MOFs), which are undesirable for biological imaging purposes.

Unlike the above fluorescent materials, carbon dots (C-dots) are a type of heavy-metal-free nanomaterial.[41–43] They have been found to have a variety of advantages that other materials do not have, for example, excitation-dependent tunable-emissions,[44] raw materials with low cost,[45] small particle size,[46] and many facile synthesis strategies.[17] Moreover, C-dots doped with other heteroatoms (*e.g.* nitrogen,[44] sulfur,[47] and boron[48]) show improved optical and electronic properties, allowing the C-dots to have broader application opportunities compared to pure C-dots.

In this work, we fabricated and reported a type of nitrogen-doped fluorescent C-dots using a one-pot hydrothermal method. In order to characterize the phase-purity, structural information and fluorescence properties of the nitrogen-doped C-dots, various techniques, such as X-ray diffraction (XRD), transmission electron microscopy (TEM), and fluorescence spectroscopy, were carried out. As a result, we found that the C-dots possess the advantages of being small in size, rich nitrogen content (28.56%), excitation-dependent tunable emissions, low cytotoxicity and good stability in water. Typically, our biological application revealed that this type of C-dots could allow us to trace, detect, localize, and distinguish between hepatoma and HeLa cells when the two cells were mixed with each other.

[a]*Shanghai University of Medicine & Health Sciences, Affiliated Sixth People's Hospital South Campus, Shanghai, China*

[b]*Department of Oncology, Humanity Hospital of Longyan City, Longyan, China*

[c]*Department of Oncology Interventional Therapy, Renji Hospital, School of Medicine, Shanghai Jiao Tong University, Shanghai, China. E-mail: scarli8880@126.com*

[d]*Department of Environmental Engineering, Zhejiang Normal University, Hangzhou 310058, China. E-mail: superfly56@126.com*

[e]*State Key Laboratory of Environmental Chemistry and Ecotoxicology, Chinese Academy of Sciences (CAS), Beijing, China*

Table 1 Nitrogen content of the obtained C-dots achieved using different content ratios (*R*) of ethylenediamine and anhydrous citric acid at different temperatures

Ethylenediamine/mL	Anhydrous citric acid/g	Temperature/°C	N content/%
40	1	140	3.75
40	3	160	10.21
40	5	180	28.56
40	7	200	24.38
40	9	240	19.59
40	5	140	21.60
40	5	160	22.67
40	5	200	26.74

2. Experimental section

2.1 Synthesis details

We prepared nitrogen doped C-dots using a one-pot hydrothermal method.[49–51] We first used 40.0 mL of distilled water to dissolve ethylenediamine and anhydrous citric acid and then transferred the dissolved solution into a 100 mL Teflon-lined autoclave, where the amounts of ethylenediamine and anhydrous citric acid used can be found in Table 1. After being treated at different temperatures (Table 1) for 2 h and then subjected to a dialysis membrane (cut-off M_n: 3.0 kDa) at room temperature for 48 h, the target brown colored nitrogen C-dots were freeze-dried under vacuum.

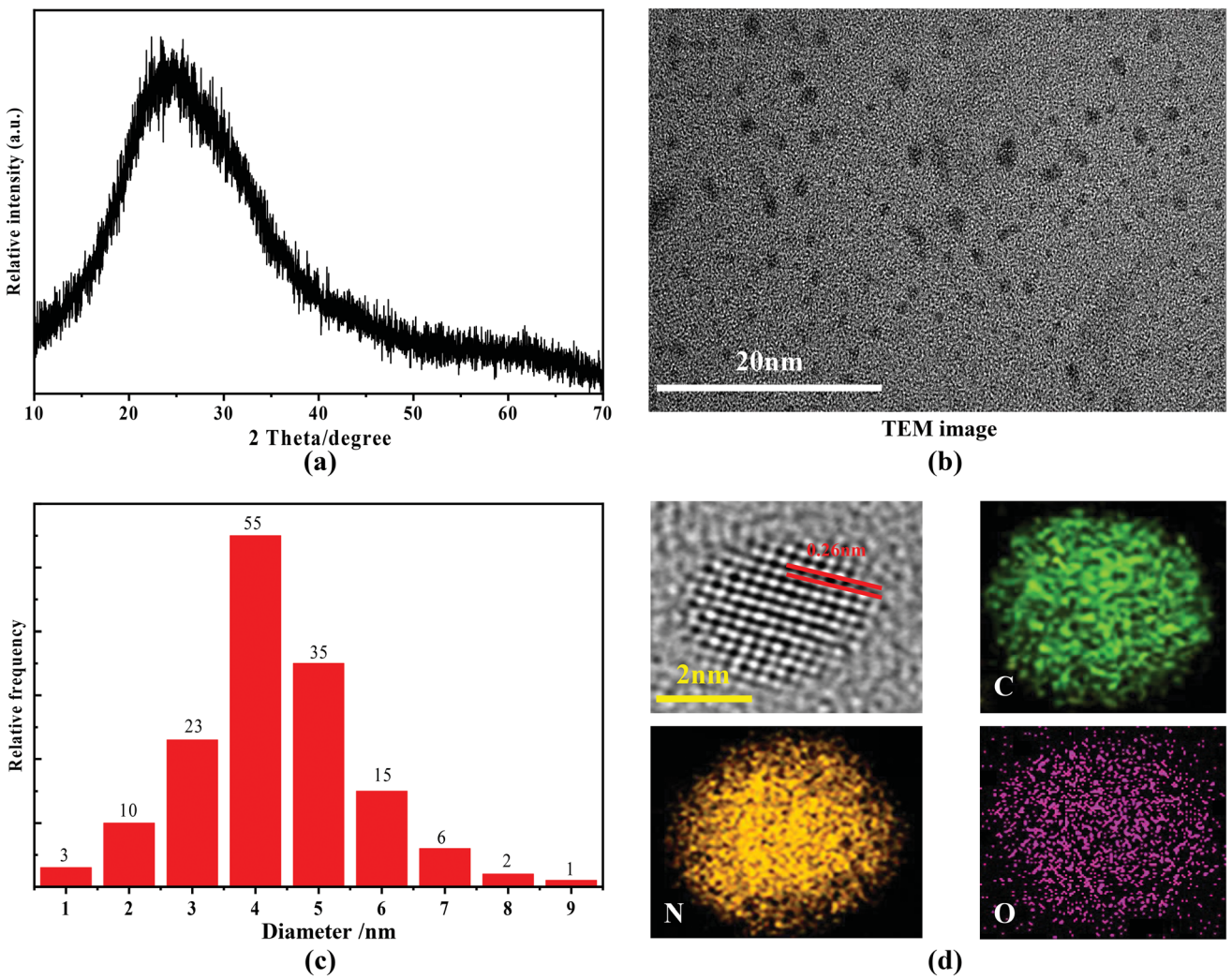

Fig. 1 (a) XRD pattern, (b) TEM image, (c) size distribution, (d) high-resolution TEM image and elemental mapping of the as-prepared nitrogen C-dots.

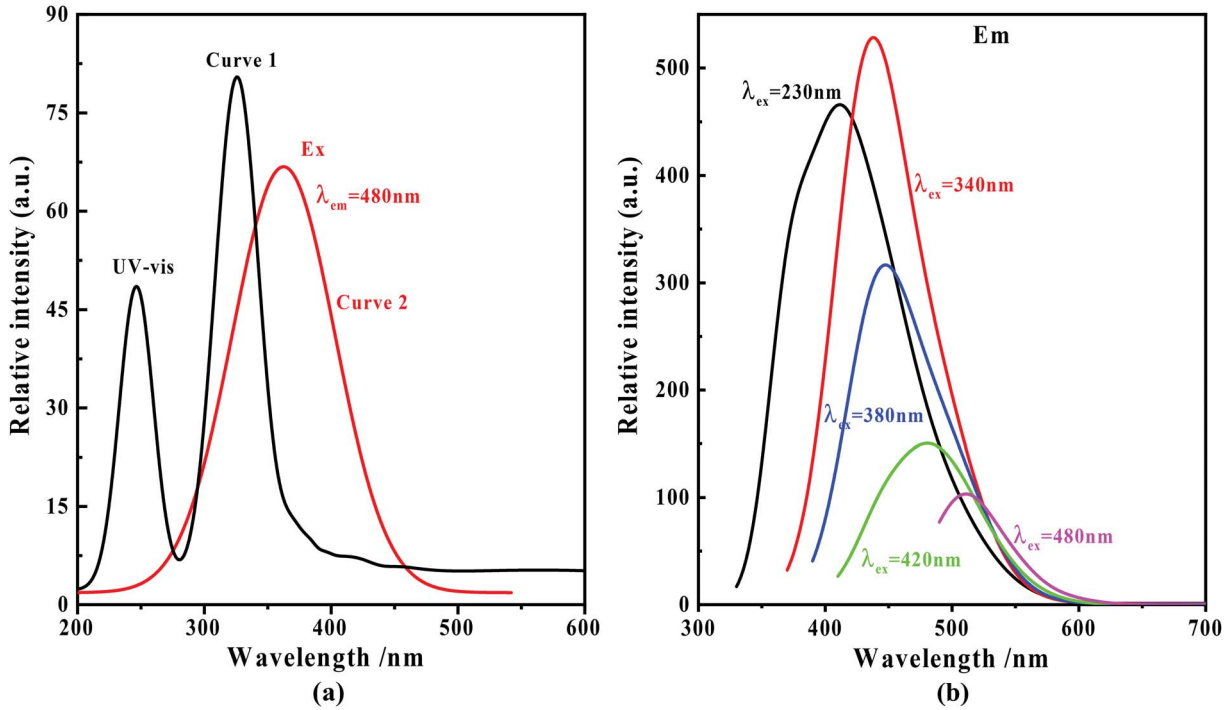

Fig. 2 (a) UV-vis absorption (curve 1) and excitation spectra (curve 2) of the nitrogen C-dots; (b) fluorescence spectra of the nitrogen C-dots upon excitation in the range of 230–480 nm.

2.2 Characterization details

The X-ray diffraction (XRD) of the nitrogen C-dots was recorded on a Bruker diffractometer utilizing Cu Kα as the radiation source ($\lambda = 1.5418$ Å). The ultraviolet-visible (UV-vis) absorption and fluorescence spectra were recorded using a PerkinElmer Lambda 25 spectrophotometer and FLS920P Edinburgh Analytical Instrument (Edinburgh Instruments), respectively. Transmission electron microscope (TEM) images were collected

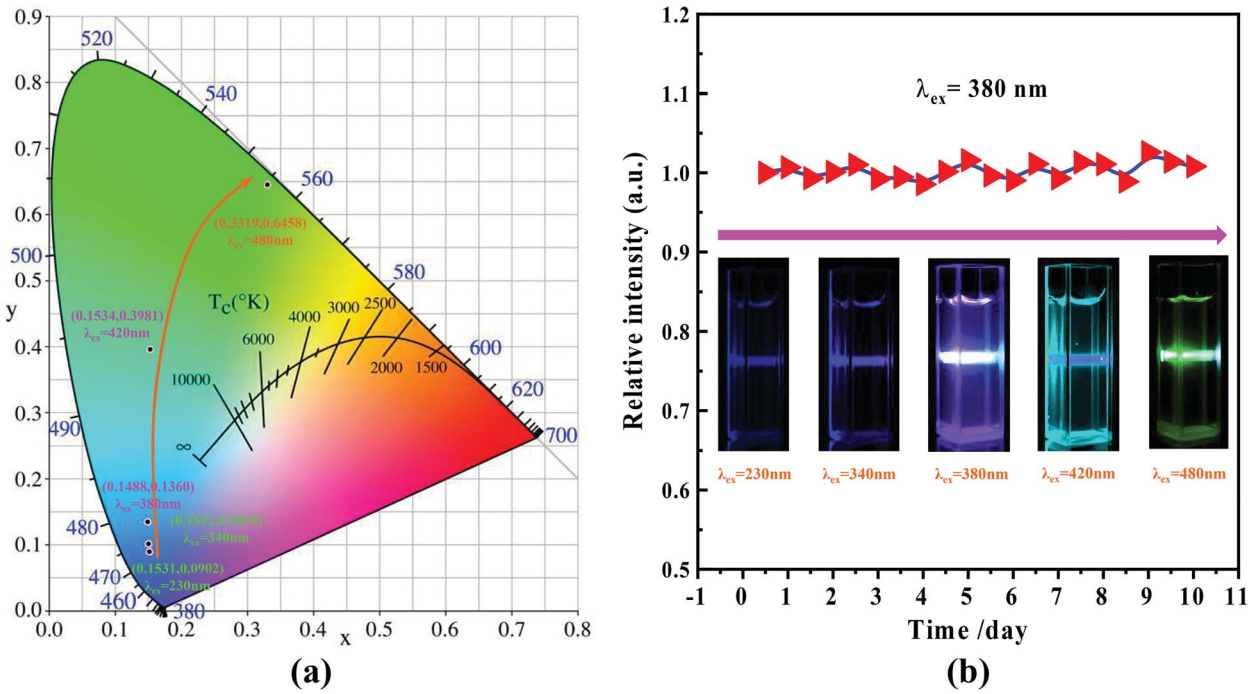

Fig. 3 (a) CIE chromaticity coordinates derived from the emission spectra in Fig. 2(b); (b) dependence of the emission intensity in terms of days ($\lambda_{ex} = 380$ nm) and digital fluorescent colors recorded by exciting with different wavelengths of light (inset).

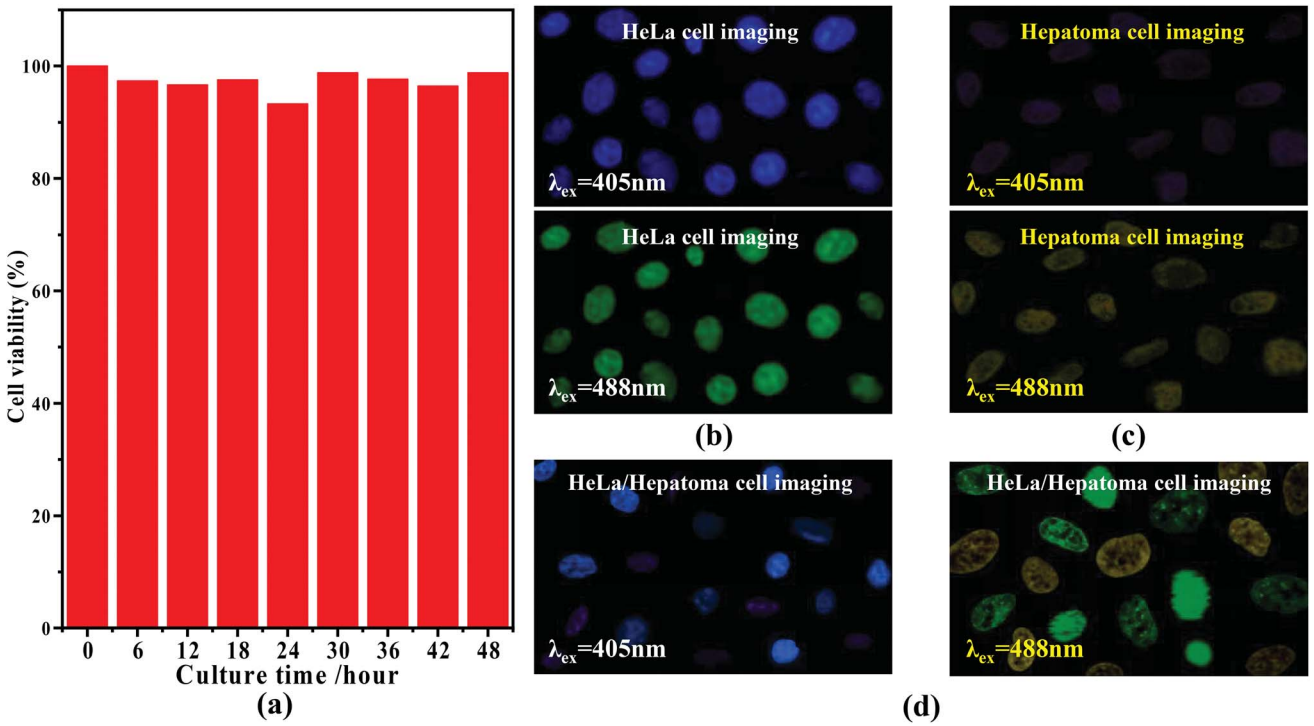

Fig. 4 (a) Viability of HeLa cells after being cultured with 1.0 mg mL^{-1} of C-dots for 48 h; (b) imaging patterns of HeLa cells upon excitation at 405 and 488 nm; (c) imaging patterns of hepatoma cells upon excitation at 405 and 488 nm; and (d) imaging patterns of HeLa-hepatoma cells upon excitation at 405 and 488 nm.

by a JEM-2100F (JEOL, Japan) instrument. The cell imaging was performed on a confocal microscopy equipped with 405 and 488 nm lasers.

3. Results and discussion

3.1 Structural analysis

The XRD pattern of the as-prepared nitrogen C-dots is shown in Fig. 1(a). A broad diffraction peak located at 23.85° is observable. This peak can be ascribed to the (002) lattice spacing that results from the diffraction of disordered carbon atoms, which can be seen in studies on other reported carbon-based materials.[41–50] The related TEM image reveals that the as-obtained C-dots are spherical dots (Fig. 1(b)) with a narrow size distribution (Fig. 1(c)). The average size of the nitrogen C-dots is ~4.6 nm. The high-resolution TEM image shows that the lattice spacing is 0.26 nm (see Fig. 1(d)), which is associated with the (100) facet of sp^2 graphitic carbon.[51,52] The elemental mapping (see Fig. 1(d)), recording from one particle of the nitrogen C-dots, confirms that the C-dots consist of N, C, and O elements. The EDS analysis shows that the maximum nitrogen content is 28.56%, which is related to the C-dots being prepared with 40 mL of ethylenediamine and 5.0 g of anhydrous citric acid at 180 °C. Such nitrogen content is higher than other nitrogen contents reported in previous works, such as, 25.1% N content in N,S-doped C-dots[53] and 18% N content in N,S-doped C-dots.[54] Such a high nitrogen content ensures that the nitrogen C-dots have good solubility in water.

3.2 UV-vis absorption and fluorescence spectral analysis

The UV-vis absorption curve of the nitrogen C-dots is shown in Fig. 2(a) (curve 1). In the figure, two absorption bands at around 244 and 323 nm, which are ascribed to the π–π* transitions of the carbonyl group (CC/CO) and n–π* transitions of the amine moiety,[51–54] are observable within the range of 200–400 nm. The absorption tail terminates at about 520 nm. In this case, we recorded the fluorescence spectra of nitrogen C-dots upon excitation in the range of 230–500 nm. As depicted in Fig. 2(b), as the excitation wavelength increases from 230 to 500 nm, the nitrogen C-dots show a regular shift in emission positions. Such excitation-dependent tunable fluorescence further results in a regular change in the Commission International d'Eclairage (CIE) chromaticity coordinates and tunable emission colors from blue to green (Fig. 3(a)). Moreover, the nitrogen C-dots, after being placed in water for 10 days, still exhibited bright fluorescence upon irradiation at 365 nm. The emission intensity is comparable to the initial emission intensity upon excitation at 365 nm (Fig. 3(b)). This indicates that this type of nitrogen C-dots holds excellent stability in aqueous solution. As shown in Fig. 2(a) (curve 2), the nitrogen C-dots exhibited one excitation band, with the maximum intensity at 380 nm, which is the reason why we use the excitation wavelength of 380 nm to record the emission intensity of Fig. 3(b).

3.3 Biological application

Based upon the florescence of Fig. 3(b) (inset), the C-dots feature a variety of emission colors upon different excitation

wavelengths. Typically, when considering semiconductor 405 and 488 nm lasers, we believe they can be used for the imaging of cells. Moreover, enlightened by the results reported by Zhu[55] and Zhou *et al.*,[56,57] it was found that different cells can exhibit different responses in their sensitivity to different fluorescence, which could allow us to use the nitrogen C-dots to trace, detect and distinguish between a given type of cell from other cells. Prior to the related experiments, we first verified the toxicity of the C-dots using HeLa cells, through mixing the C-dots and HeLa cells and then monitored the survival viability of the HeLa cells. As shown in Fig. 4(a), we observed that HeLa cells after being cultured with 1.0 mg mL^{-1} of C-dots for 48 h exhibit viability analogous to the comparative HeLa cells without C-dots. The viability of the HeLa cells after being cultured for 48 h remained at more than 97%, indicating that the nitrogen C-dots exhibit low cytotoxicity and thus can be used for cell imaging. As revealed in Fig. 4(b), upon excitation at 405 and 488 nm, two colors, as shown in the digital images, are observable in the C-dot-stained HeLa cells. The results in Fig. 4(b) reveal that the nitrogen C-dots successfully entered into the membrane and cytoplasmic area of the HeLa cells. Furthermore, such fluorescent colors are also suitable for imaging other cells such as hepatoma cells (Fig. 4(c)). However, the hepatoma cells show different imaging colors from those of the HeLa cells, where the imaging colors excited at 405 and 488 nm are purple and yellow, respectively. In view of this, we proposed to distinguish between hepatoma and HeLa cells when the two types of cells were mixed with each other. We first mixed 10 μL of HeLa cells and 10 μL of hepatoma cells and then injected 10 μL of 1.0 mg L^{-1} C-dots into the mixed cells. As shown in Fig. 4(d), we observed two types of different fluorescent colors that correspond to the two types of cells. More specifically, upon excitation at 405 and 488 nm, the C-dot-cultured HeLa cells exhibit blue and green colors, which are the same as shown in Fig. 4(b). However, the hepatoma cells exhibit purple and yellow colors analogous to those shown in Fig. 4(c). Obviously, we have used the nitrogen C-dots as a type of imaging probe technique to trace, detect and distinguish between hepatoma and HeLa cells based upon the different sensitivities of the different cells to different fluorescence.

4. Conclusions and outlook

In this work, nitrogen rich C-dots were prepared using a one-pot hydrothermal method. We revealed that the maximum nitrogen content of the C-dots was as high as 28.56%. With an increase in the excitation wavelength from 230 to 520 nm, excitation-dependent fluorescence from blue to green was observable for the nitrogen rich C-dots. With the features of being small in size, having good stability in water and low cytotoxicity, as well as excitation-dependent tunable fluorescence, we found that the HeLa cells after being cultured with C-dots exhibited blue and yellow fluorescence upon excitation at 405 and 488 nm, analogous to the colors exhibited in aqueous solution, respectively. Moreover, based upon the behavior that involves the different sensitivities of different cells to different fluorescence, by using the C-dots, we were able to trace, detect and distinguish between hepatoma and HeLa cells.

Actually, the underlying reasons for the above observation after an in-depth consideration are very complicated, which can be related to a lot of potential mechanisms that can lead to the change of fluorescent colors in the as-obtained carbon dots. On the one hand, such a difference may be due to the unique protein properties of each of the cells and their different extent of C-dot accumulation. The C-dots exhibit different colors when they have different accumulations. In addition, this may also be because the proteins of the different cells are sensitive to their surrounding environments. Furthermore, since the particle size of the C-dots can influence the fluorescent colors. A smaller size is usually related to blue fluorescence, while a bigger size is related to red fluorescence. In this case, we also deduced that different types of cells may absorb different sizes of C-dots, leading to the different fluorescence of the cells. Although we have only so far demonstrated that two types of cells can exhibit these results when mixed together, we believe that there is the potential for other types of cells to also exhibit this behavior. This is a new, yet exciting, observation, which needs further study in the future in order to understand the underlying reasons behind this behavior. This work shows that C-dots can not only be used for biomedical imaging, but can also be used as an effective, low cost and non-invasive detection method to trace and distinguish between hepatoma and HeLa cells.

Conflicts of interest

The authors declare that they have no conflicts of interest with the contents of this article.

References

1 L. Kelland, *Nat. Rev. Cancer*, 2007, **7**, 573–584.
2 K. H. Bae, M. Park, M. J. Do, N. Lee, J. H Ryu, G. W. Kim, C. Kim, T. G. Park and T. Hyeon, *ACS Nano*, 2012, **6**, 5266–5273.
3 T. Kobayashi, *Biotechnol. J.*, 2011, 61342–61347.
4 Z. J. Zhang, J. Wang and C. Y. Chen, *Adv. Mater.*, 2013, **25**, 3869–3880.
5 Z. Xiao, C. Ji, J. Shi, E. M. Pridgen, J. Frieder, J. Wu and O. C. Farokhzad, *Angew. Chem., Int. Ed.*, 2012, **51**, 11853–11857.
6 M. Yu, F. Guo, F. Tan and N. Li, *J. Controlled Release*, 2015, **215**, 91–100.
7 A. Hervault and N. T. K. Thanh, *Nanoscale*, 2014, **6**, 11553–11573.
8 P. Pradhan, J. Giri, F. Rieken, C. Koch, O. Mykhaylyk, M. Döblinger, R. Banerjee, D. Bahadur and C. Plank, *J. Controlled Release*, 2010, **142**, 108–121.
9 R. R. Love, H. Leventhal, D. V. Easterling and D. R. Nerenz, *Cancer*, 1989, **63**, 604–612.
10 A. H. Partridge, H. J. Burstein and E. P. Winer, *JNCI Monogr.*, 2001, **2001**, 135–142.

11 A. I. Buizer, L. M. J. de Sonneville, M. M. van den Heuvel-Eibrink and A. J. P. Veerman, *Pediatr. Blood Cancer*, 2005, **42**, 281.
12 T. S. Hauck, T. L. Jennings, T. Yatsenko, J. C. Kumaradas and W. C. W. Chan, *Adv. Mater.*, 2008, **20**, 3832–3838.
13 L. Yuan, W. Y. Lin, K. B. Zheng, L. W. He and W. M. Huang, *Chem. Soc. Rev.*, 2013, **42**, 622–661.
14 X. Y. Zhang, X. Q. Zhang, B. Yang, M. Y. Liu, W. Y. Liu, Y. W. Chen and Y. Wei, *Polym. Chem.*, 2013, **4**, 4317–4321.
15 U. Resch-Genger, M. Grabolle, S. Cavaliere-Jaricot, R. Nitschke and T. Nann, *Nat. Methods*, 2008, **5**, 763–775.
16 Z. M. Tao, G. S. Hong, C. Shinji, C. X. Chen, S. Diao, A. L. Antaris, B. Zhang, Y. P. Zou and H. J. Dai, *Angew. Chem., Int. Ed.*, 2013, **52**, 13002–13006.
17 A. W. Wang, F. W. Kang, Z. G. Wang, Q. G. Shao, Z. Li, G. Y. Zhu, J. Lu and Y. Y. Li, *Adv. Sustainable Syst.*, 2019, **3**, 1800132.
18 I. L. Medintz, H. T. Uyeda, E. R. Goldman and H. Mattoussi, *Nat. Mater.*, 2005, **4**, 435–446.
19 J. K. Jaiswal, H. Mattoussi, J. M. Mauro and S. M. Simon, *Nat. Biotechnol.*, 2003, **21**, 47–51.
20 A. M. Smith, H. W. Duan, A. M. Mohs and S. M. Nie, *Adv. Drug Delivery Rev.*, 2008, **60**, 1226–1240.
21 C. F Wu, B. Bull, C. Szymanski, K. Christensen and J. McNeill, *ACS Nano*, 2008, **2**, 2415–2423.
22 K. Y. Pu, A. J. Shuhendler, J. V. Jokerst, J. G. Mei, S. S. Gambhir, Z. N. Bao and J. H. Rao, *Nat. Nanotechnol.*, 2014, **9**, 233–239.
23 K. Li and B. Liu, *Chem. Soc. Rev.*, 2014, **43**, 6570–6597.
24 S. A. Jones, S.-H. Shim, J. He and X. W. Zhuang, *Nat. Methods*, 2011, **8**, 499–505.
25 V. Emiliani, D. Sanvitto and M. Tramier, *Appl. Phys. Lett.*, 2003, **83**, 2471.
26 L. H. V. Wang, X. M. Zhao, H. T. Sun and G. Ku, *Rev. Sci. Instrum.*, 1999, **70**, 3744.
27 N. Terasaki, H. W. Zhang, H. Yamada and C.-N. Xu, *Chem. Commun.*, 2011, **47**, 8034–8036.
28 C. M. Lau, X. W. Xu and K. W. Kwok, *Appl. Surf. Sci.*, 2015, **336**, 314–320.
29 Y. T. Zhong, Z. R. Ma, S. J. Zhu, J. Y. Yue, M. X. Zhang, A. L. Antaris, J. Yuan, R. Cui, H. Wan, Y. Zhou, W. Z. Wang, N. F. Huang, J. Luo, Z. Y. Hu and H. J. Dai, *Nat. Commun.*, 2017, **8**, 737.
30 H. F. Dong, S. S. Tang, Y. S. Hao, H. Z. Yu, W. H. Dai, G. F. Zhao, Y. Cao, H. T. Lu, X. J. Zhang and H. X. Ju, *ACS Appl. Mater. Interfaces*, 2016, **8**, 3107–3114.
31 G. Brida, M. Genovese and I. R. Berchera, *Nat. Photonics*, 2010, **4**, 227–230.
32 L. L. Li, P. W. Wu, K. Hwang and Y. Lu, *J. Am. Chem. Soc.*, 2013, **135**, 2411–2414.
33 M. X. Yu, F. Y. Li, Z. G. Chen, H. Hu, C. Zhan, H. Yang and C. H. Huang, *Anal. Chem.*, 2019, **81**, 930–935.
34 H. C. Lu, G. S. Yi, S. Y. Zhao, D. P. Chen, L.-H. Guo and J. Cheng, *J. Mater. Chem.*, 2004, **14**, 1336–1341.
35 F. W. Kang, J. J. He, T. Y. Sun, Z. Y. Bao, F. Wang and D. Y. Lei, *Adv. Funct. Mater.*, 2017, **27**, 1701842.
36 Q. Q. Miao, C. Xie, X. Zhen, Y. Lyu, H. W. Duan, X. G. Liu, J. V. Jokerst and K. Y. Pu, *Nat. Biotechnol.*, 2017, **35**, 1102–1110.
37 C. Xie, X. Zhen, Q. Q. Miao, Y. Lyu and K. Y. Pu, *Adv. Mater.*, 2018, **30**, 1801331.
38 X. Zhen, Y. Tao, Z. F. An, P. Chen, C. J. Xu, R. F. Chen, W. Huang and K. Y. Pu, *Adv. Mater.*, 2017, **29**, 1606665.
39 P. Horcajada, T. Chalati, C. Serre, B. Gillet, C. Sebrie, T. Baati, J. F. Eubank, D. Heurtaux, P. Clayette, C. Kreuz, J.-S. Chang, Y. K. Hwang, V. Marsaud, P.-N. Bories, L. Cynober, S. Gil, G. Férey, P. Couvreur and R. Gref, *Nat. Mater.*, 2010, **9**, 172–178.
40 K. M. L. Taylar, A. Jin and W. B. Lin, *Angew. Chem., Int. Ed.*, 2008, **47**, 7722–7725.
41 A. W. Wang, Y.-L. Hou, F. W. Kang, F. C. Lyu, Y. Xiong, W.-C. Chen, C.-S. Lee, Z. T. Xu, A. L. Rogach, J. Lu and Y. Y. Li, *J. Mater. Chem. C*, 2019, **7**, 2207.
42 Z. N. Tan, Y. Zhang, C. Xie, H. P. Su, J. Liu, C. F. Zhang, N. Dellas, S. E. Mohney, Y. Q. Wang, J. K. Wang and J. Xu, *Adv. Mater.*, 2011, **23**, 3553–3558.
43 C. X. Wang, Z. Z. Xu, H. Cheng, H. H. Lin, M. G. Humphrey and C. Zhang, *Carbon*, 2015, **82**, 87–95.
44 D. Qu, M. Zheng, J. Li, Z. G. Xie and Z. C. Sun, *Light: Sci. Appl.*, 2015, **4**, e364.
45 K. Jiang, L. Zhang, J. F. Lu, C. X. Xu, C. Z. Cai and H. W. Lin, *Angew. Chem., Int. Ed.*, 2016, **55**, 7231–7235.
46 K. Jiang, S. Sun, L. Zhang, Y. Lu, A. G. Wu, C. Z. Cai and H. W. Lin, *Angew. Chem., Int. Ed.*, 2015, **54**, 5360–5363.
47 Y. Q. Dong, H. C. Pang, H. B. Yang, C. X. Guo, J. W. Shao, Y. W. Chi, C. M. Li and T. Yu, *Angew. Chem., Int. Ed.*, 2013, **52**, 7800–7804.
48 H. L. Fei, R. Q. Ye, G. Ye, Y. J. Gong, Z. W. Peng, X. J. Fan, E. L. G. Samuel, P. M. Ajayan and J. M. Tour, *ACS Nano*, 2014, **8**, 10837–10843.
49 T. Tian, Y. He, Y. L. Ge and G. W. Song, *Sens. Actuators, B*, 2017, **240**, 1265–1271.
50 W.-J. Niu, Y. Li, R.-H. Zhu, S. Shan, Y.-R. Fan and X.-J. Zhang, *Sens. Actuators, B*, 2015, **218**, 229–236.
51 H. Ming, Z. Ma, Y. Liu, K. M. Pan, H. Yu, F. Wang and Z. H. Kang, *Dalton Trans.*, 2012, **41**, 9526–9531.
52 C. J. Reckmeier, J. Schneider, A. S. Susha and A. L. Rogach, *Opt. Express*, 2016, **2**, A312–A340.
53 D. Sun, R. Ban, P.-H. Zhang, G.-H. Wu, J.-R. Zhang and J.-J. Zhu, *Carbon*, 2013, **64**, 424–434.
54 S. J. Zhao, M. H. Lan, X. Y. Zhu, H. T. Xue, T.-W. Ng, X. M. Meng, C.-S. Lee, P. F. Wang and W. J. Zhang, *ACS Appl. Mater. Interfaces*, 2015, **7**, 17054–17060.
55 P. C. Zhu, D. D. Lyu, P. K. Shen and X. X. Wang, *J. Lumin.*, 2019, **207**, 620–625.
56 K. Zhou, Y. Zhang, Z. N. Xia and W. L. Wei, *Nanotechnology*, 2016, **27**, 275101.
57 R. J. Liu, L. L. Zhang, Y. Y. Chen, Z. R. Huang, Y. Huang and S. L. Zhao, *Anal. Chem.*, 2018, **90**, 4452–4460.